Supporting Information

Enhanced thermoelectric performance of Mg_3Sb_2-based materials by B and Te codoping

Lijun Zhai[a,b], Jian Wang[c], Lin Cheng[a,b], Minghao Lv[a,b], Lu Gao[a,b], Zhongyuan Yang[a,b], Yanli Li[d], Yan Zhang[a,b], Hongxia Liu [a,b,*], Zhigang Sun[a,b,*]

[a] School of Materials Science & Engineering, Taiyuan University of Science and Technology, Taiyuan, 030024, China

[b] Laboratory of Magnetic and Electric Functional Materials and the Applications, The Key Laboratory of Shanxi Province, Taiyuan 030024, China

[c] Hubei Longzhong Laboratory, Wuhan University of Technology Xiangyang Demonstration Zone, Xiangyang 441000, China

[d] Department of Physics, School of Science, Wuhan University of Technology, Wuhan, Hubei 430070, China

*Corresponding author. E-mail: hongxliu@tyust.edu.cn (Hongxia Liu) and sunzg@tyust.edu.cn (Zhigang Sun)

Table SI. **Measured density of $Mg_{3.2}SbBi_{1-x}Te_x$ (x=0, 0.01, 0.02, 0.03, 0.04) and $Mg_{3.2}B_ySbBi_{0.97}Te_{0.03}$ (y=0.01, 0.03, 0.05) samples.**

Compositions	Measured density (g/cm^3)	Theoretical density (g/cm^3)	Relative density
x=0, y=0	4.8	5.069	95%
x=0.01, y=0	4.89	5.024	97%
x=0.02, y=0	4.82	5.026	96%
x=0.03, y=0	4.87	5.020	97%
x=0.04, y=0	4.87	5.015	97%
x=0.03, y=0.01	4.84	5.026	96%
x=0.03, y=0.03	4.89	5.010	98%
x=0.03, y=0.05	4.89	5.025	96%

1. The fractured surface feature of $Mg_{3.2}B_{0.03}SbBi_{0.97}Te_{0.03}$ bulk sample

SEM images of the freshly fractured surface morphology of $Mg_{3.2}B_{0.03}SbBi_{0.97}Te_{0.03}$ bulk sample in Fig. S1. (a) and the right column of Fig. S1. (b) is an enlarged view of the selected locally area. It can be seen that the sample has a typical layered structure with the grain size is about 10 μm, and each grain is composed of many nanolayers without obvious cracks or pores.

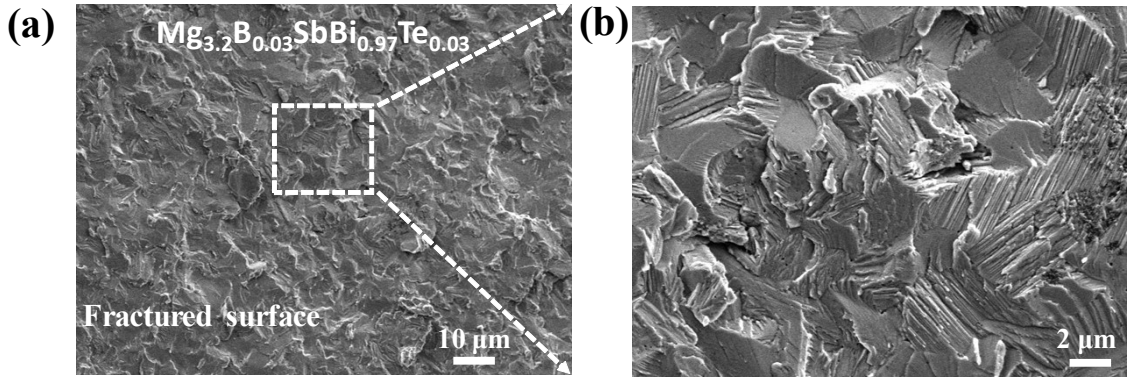

Fig. S1. (a) SEM image of fractured surface of $Mg_{3.2}B_{0.03}SbBi_{0.97}Te_{0.03}$ bulk sample and (b) the magnified SEM image taken from (a).

2. Electronic thermal conductivity of $Mg_{3.2}SbBi_{1-x}Te_x$ (x = 0, 0.01, 0.02, 0.03, 0.04) samples.

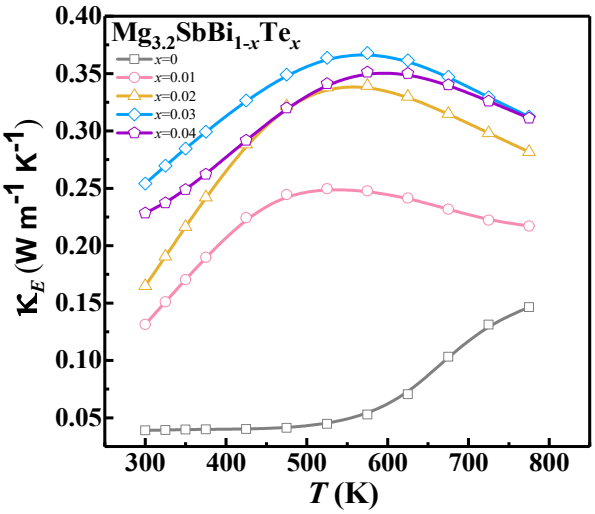

Fig. S2 Temperature dependent electronic thermal conductivity of $Mg_{3.2}SbBi_{1-x}Te_x$ (x = 0, 0.01, 0.02, 0.03, 0.04) samples.

3. Thermal diffusivities of $Mg_{3.2}SbBi_{1-x}Te_x$ (x = 0, 0.01, 0.02, 0.03, 0.04) and $Mg_{3.2}B_ySbBi_{0.97}Te_{0.03}$ (y = 0.01, 0.03, 0.05) samples.

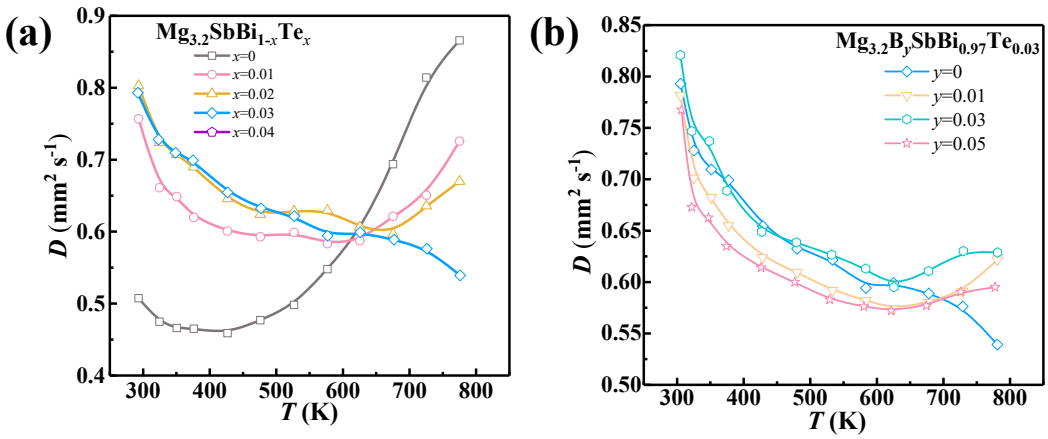

Fig. S3 (a) Thermal diffusivities of $Mg_{3.2}SbBi_{1-x}Te_x$ and (b) $Mg_{3.2}B_ySbBi_{0.97}Te_{0.03}$ samples.

4. Comparison of zT of $Mg_{3.2}SbBi_{1-x}Te_x$ samples with other high-performance n-type Mg_3Sb_2 materials.

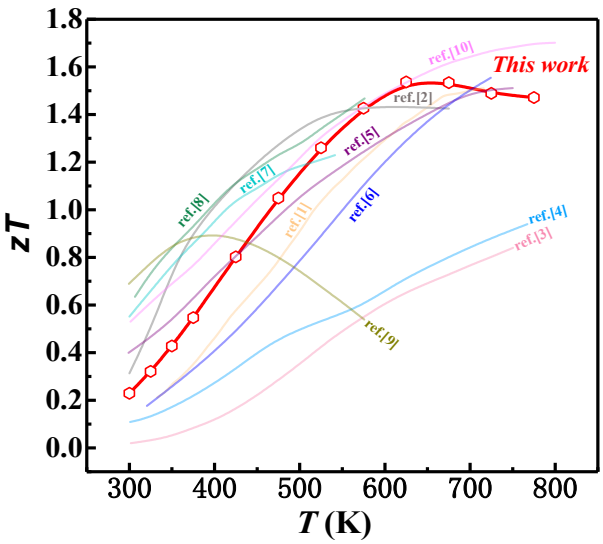

Fig. S4 Comparison of zT of $Mg_{3.2}SbBi_{1-x}Te_x$ samples obtained in this work with those of other high-performance n-type Mg_3Sb_2 materials [1-10].

4. Calculated physical properties of all samples

The physical parameters such as the average sound velocity (v_S), Debye temperature (θ_D), Poisson's ratio (v_p), bulk modulus (B), and Grüneisen constant (γ) are given by formulas S1-S5, respectively[11-13]. Here, v_T, v_L, $\hbar$, k_B and n_a represent the transverse wave velocity, longitudinal wave velocity, Planck constant, Boltzmann constant and the number of atoms per unit volume, respectively, and d is the density obtained from the test.

$$v_S = \left[\frac{1}{3}\left(\frac{2}{v_T^{\,3}} + \frac{1}{v_L^{\,3}}\right)\right]^{-1/3} \tag{S1}$$

$$\theta_D = v_S \frac{h}{k_B}\left(6\pi^2 n_a\right)^{1/3} \tag{S2}$$

$$v_p = \frac{3B - 2dv_T^{\,2}}{6B + 2dv_T^{\,2}} \tag{S3}$$

$$B = \frac{d(3v_L^{\,2} - 4v_T^{\,2})}{3} \tag{S4}$$

$$\gamma = \frac{3}{2}\frac{3v_L^{\,2} - 4v_T^{\,2}}{v_L^{\,2} + 2v_T^{\,2}} \tag{S5}$$

5. Quality factor *B* for $Mg_{3.2}B_ySbBi_{0.97}Te_{0.03}$ (y = 0.01, 0.03, 0.05) samples.

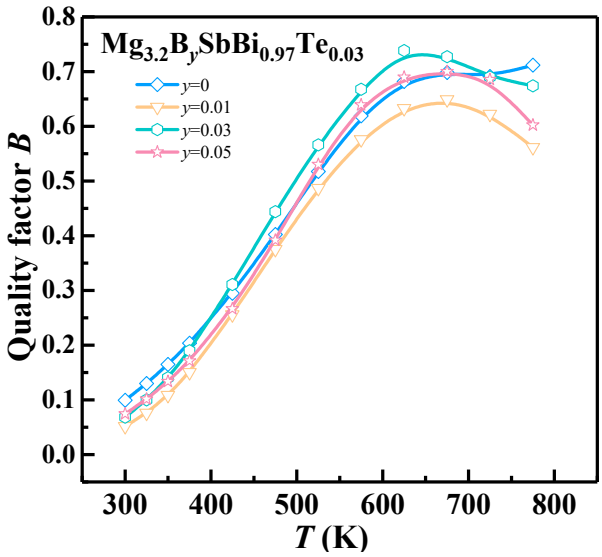

Fig. S5 Quality factor *B* for $Mg_{3.2}B_ySbBi_{0.97}Te_{0.03}$ (y = 0.01, 0.03, 0.05) samples.

References:

1. R. Shu, Y. Zhou, Q. Wang, Z. Han, Y. Zhu, Y. Liu, Y. Chen, M. Gu, W. Xu, Y. Wang, W. Zhang, L. Huang and W. Liu, *Advanced Functional Materials*, 2019, **29**, 1807235.
2. X. Yang, H. Ni, X. Yu, B. Cao, J. Xing, Q. Chen, L. Xi, J. Liu, J. Zhang, K. Guo and J.-T. Zhao, *Journal of Materiomics*, 2023, **10**, 154-162.
3. S. Ohno, K. Imasato, S. Anand, H. Tamaki, S. D. Kang, P. Gorai, H. K. Sato, E. S. Toberer, T. Kanno and G. J. Snyder, *Joule*, 2018, **2**, 141-154.
4. J. I. Tani and H. Ishikawa, *Journal of Materials Science: Materials in Electronics*, 2020, **31**.
5. J. Lei, H. Wuliji, K. Zhao, T. R. Wei, Q. Xu, P. Li, P. Qiu and X. Shi, *Journal of Materials Chemistry A*, 2021, **9**, 25944-25953.
6. L. Yu, W. Li, Z. Zhang, S. Wei, J. Li, Z. Ji, J. Zhuo, G. Lu, W. Song and S. Zheng, *Materials Today Physics*, 2022, **26**, 100721.
7. X. Shi, C. Sun, X. Zhang, Z. Chen, S. Lin, W. Li and Y. Pei, *Chemistry of Materials*, 2019, **31**, 8987-8994.
8. Z. Liang, C. Xu, H. Shang, M. Ning, T. Tong, S. Song, W. Ren, X. Shi, X. Liu, F. Ding, J. Bao, D. Wang and Z. Ren, *Advanced Energy Materials*, 2023, **13**, 2301107.
9. K. Imasato, S. D. Kang and G. J. Snyder, *Energy & Environmental Science*, 2019, **12**, 965-971.
10. X. Shi, T. Zhao, X. Zhang, C. Sun, Z. Chen, S. Lin, W. Li, H. Gu and Y. Pei, *Adv Mater*, 2019, **31**, 1903387.
11. O. L. Anderson, *Journal of Physics and Chemistry of Solids*, 1963, **24**, 909-917.
12. P. H. Mott, J. R. Dorgan and C. M. Roland, *Journal of Sound and Vibration*, 2008, **312**, 572-575.
13. D. S. Sanditov and V. N. Belomestnykh, *Technical Physics*, 2011, **56**, 1619-1623.